Chapter 17
Xanthorhodopsin

Janos K. Lanyi and Sergei P. Balashov

17.1 Introduction

The extremely halophilic Archaea have acquired a capability for phototrophy based on a single protein with an attached retinal chromophore. It captures light and utilizes the energy gained by performing transmembrane ion transfer to generate electrochemical gradients (Drachev et al. 1976; Michel and Oesterhelt 1980) that are used for ATP synthesis, motility, and transport. The classical examples are bacteriorhodopsin, the proton pump of *Halobacterium salinarum* (Oesterhelt and Stoeckenius 1973), and halorhodopsin, the light driven chloride pump (Schobert and Lanyi 1982). This type of simple energy transducer and light sensor was a very useful "invention" early in evolution, and it has spread far beyond the halophilic world in the form of the homologous proteorhodopsins found in the genomes of eubacteria, inhabiting sea waters (Béjà et al. 2000, 2001; Venter et al. 2004; Gomez-Consarnau et al. 2007) and fresh waters (Sharma et al. 2009). They are present in an ancient Siberian permafrost (Petrovskaya et al. 2010), and were found in many eukaryotes as well (Brown and Jung 2006). Xanthorhodopsin (Balashov et al. 2005) was discovered in and isolated from a cultured extremely halophilic eubacterium, *Salinibacter ruber,* which shares its environment with haloarchaea (Antón et al. 2002). It was soon recognized that, besides xanthorhodopsin, its genome contains three other retinal proteins, one homologous to halorhodopsin (Peña et al. 2005) and two sensory rhodopsins (Mongodin et al. 2005). Xanthorhodopsin is unique in that it has a light-harvesting antenna in addition to retinal.

Photosynthetic systems in biology depend on specialized colored molecules that are suitable both for collecting light and converting the absorbed electromagnetic energy into usable forms. Because of chemical constraints, these requirements are not always both optimally achieved, and the chromophores in reaction centers are often supplemented by auxiliary pigments, which harvest light and funnel energy to

J.K. Lanyi (✉) • S.P. Balashov
Department of Physiology & Biophysics, University of California, Irvine, CA 92697, USA
e-mail: jklanyi@uci.edu

A. Ventosa et al. (eds.), *Halophiles and Hypersaline Environments*,
DOI 10.1007/978-3-642-20198-1_17,

the center. Chlorophyll-based photosynthesis utilizes carotenoids and other pigments in large multi-chromophore protein complexes as antennae (McDermott et al. 1995; Polívka and Frank 2010). Bacteriorhodopsin of *Halobacterium salinarum*, a much simpler energy transducer, does not have such an antenna (Oesterhelt and Stoeckenius 1973; Litvin et al. 1977) whereas xanthorhodopsin contains a carotenoid, salinixanthin (Lutnaes et al. 2002), serving as antenna. Other than being a dual-chromophore system (with one retinal and one carotenoid molecule), this small heptahelical transmembrane protein (Balashov et al. 2005; Luecke et al. 2008) is similar to bacteriorhodopsin and especially its eubacterial counterparts, the proteorhodopsins (Béjà et al. 2000, 2001). Much is known already about this protein. Action spectra indicated that both chromophores participate in driving proton transport (Balashov et al. 2005; Boichenko et al. 2006), and the observed dependence of a tight and specific carotenoid binding on the presence of retinal (Balashov et al. 2005, 2006; Imasheva et al. 2008) suggested their close interaction. Recent steady-state and ultrafast spectroscopy confirmed the postulated energy transfer from the excited state of the carotenoid to the retinal, and described features of the excited states involved (Balashov et al. 2008; Polívka et al. 2009; Zhu et al. 2010). The deduced geometry of the two polyene chains from spectroscopic data (Balashov et al. 2008) is consistent with the recently solved crystal structure of the protein (Luecke et al. 2008), the first one for an eubacterial proton pump. The structure revealed not only the precise location of the carotenoid antenna but also entirely new features in architecture of the proton conducting pathways, especially on the extracellular side where proton release takes place. It is probable that these structural features are present in many eubacterial retinal proteins, proteorhodopsins and other proteins homologous to xanthorhodopsin.

The genome of *Salinibacter ruber* and the relationship of the xanthorhodopsin gene to other retinal proteins (Fig. 17.1a) were described (Mongodin et al. 2005). Alignment of the amino acid sequences indicates that xanthorhodopsin has slightly higher homology to proteorhodopsins than to bacteriorhodopsin (61 identities vs. 58, Fig. 17.1b). A xanthorhodopsin-like gene was found in an abundant coastal ocean methylotroph that utilizes methanol and formaldehyde as sources of carbon (Giovannoni et al. 2008). This gene forms a clade with the xanthorhodopsin of *Salinibacter ruber* and the rhodopsins of cyanobacterium *Gloeobacter violaceus* and the dinoflagellate *Pyrosystis lunula*, and homologous to several other divergent organisms (Sharma et al. 2008; Imasheva et al. 2009). It appears that xanthorhodopsin-like retinal proteins might be as widespread and numerous as the homologous proteorhodopsins (Béjà et al. 2001; Fuhrman et al. 2008).

This review examines current issues concerning xanthorhodopsin as a simple dual-chromophore system for absorption and utilization of light. The outstanding questions include the structure of eubacterial proton pump, the way the large carotenoid salinixanthin (Fig. 17.2) is accommodated by the relatively small protein, the mechanism of inter-chromophore excitation energy transfer, and the distinctive features of xanthorhodopsin in comparison with the earlier studied bacteriorhodopsin and archaerhodopsin of the halobacteria and the proteorhodopsins of marine bacteria. For background material, the reader is directed to

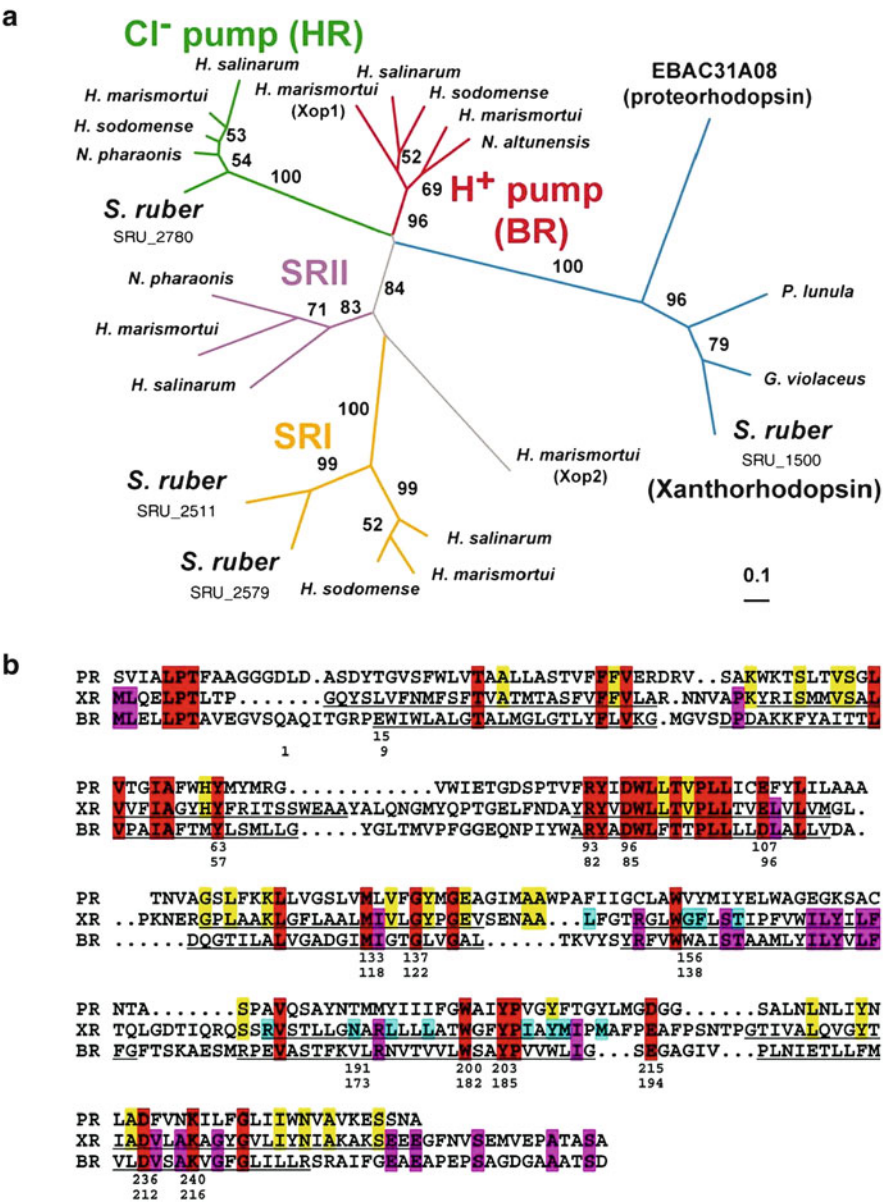

Fig. 17.1 (**a**) A likelihood phylogeny of retinal protein genes of *Salinibacter ruber*. Note the distant relationship of xanthorhodopsin to the archaeal proton pump bacteriorhodopsin, and the much greater homology to the rhodopsins of *Gloeobacter violaceus*. Three other genes in *S. ruber*, halorhodopsin (HR) and two sensory rhodopsin-I like proteins (SRI), are nearer their archaeal homologues and imply lateral gene transfer. From Mongodin et al. (2005). (**b**) Alignment of amino acid sequences of xanthorhodopsin (XR), proteorhodopsin (PR) and bacteriorhodopsin (BR). Red, residues conserved in all three proteins; yellow, conserved in PR and XR; purple, conserved in XR and BR; cyan, residues involved in carotenoid binding. *Top row* of numbers refer to the XR sequence; *bottom row*, to the BR sequence. From Luecke et al. (2008)

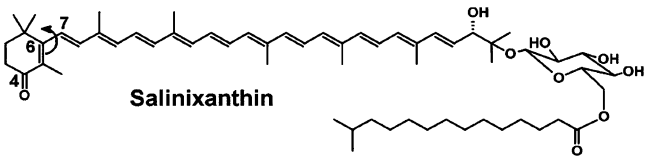

Fig. 17.2 Chemical structure of carotenoid salinixanthin from the cell membrane of *Salinibacter ruber*. From Lutnaes et al. (2002). An *arrow* around C6–C7 bond illustrates the turn of the ring in the xanthorhodopsin binding site as shown in (Balashov et al. 2006; Luecke et al. 2008)

earlier review articles on microbial retinal proteins (Oesterhelt 1998; Spudich and Jung 2005), bacteriorhodopsin (Balashov and Lanyi 2006; Hirai et al. 2009), proteorhodopsins (Fuhrman et al. 2008), xanthorhodopsin (Balashov and Lanyi 2007; Lanyi and Balashov 2008) and carotenoid antennae in different photosynthetic systems including xanthorhodopsin (Polívka and Frank 2010).

17.2 Action Spectrum of Xanthorhodopsin in Live *Salinibacter ruber* Cells

The first evidence for involvement of salinixanthin in proton transport was from measurements of action spectra for light-induced pH changes in vesicles produced by sonication of *Salinibacter ruber* cells (Balashov et al. 2005) and oxygen consumption in live cells (Balashov et al. 2005; Boichenko et al. 2006). The latter approach produced an especially detailed spectrum. Illumination of *Salinibacter ruber* cells causes decrease of respiration rate up to 50% (detected as increase in steady-state oxygen content of cell suspensions) from back-pressure of the light-induced proton electrochemical potential created by xanthorhodopsin on the electron transfer steps in the respiratory chain (Boichenko et al. 2006). Under excitation with single flashes the change in respiration rate occurred with a 0.2 s time constant, consistent with the turnover of the xanthorhodopsin photocycle (100–200 ms). The action spectrum for photoinhibition of respiration in *Salinibacter ruber* cells at high spectral resolution (4 nm) indicated participation of the carotenoid in proton pumping. The high accuracy of the spectrum made it possible to deconvolute it into two components: retinal and carotenoid (Fig. 17.3a). The derived spectrum of the carotenoid component is particularly useful for estimations of the efficiency of the antenna (ca. 40%), since the *Salinibacter* cell membrane preparations always contain a variable fraction of carotenoid unbound to xanthorhodopsin, which complicates determination of the exact spectrum of the bound component when using absorption spectroscopy.

Measurements of action spectra in archaeon *Halorubrum* sp. A1C cells containing another proton pump, archaerhodopsin (Mukohata et al. 1991), and the carotenoid bacterioruberin (Britton et al. 2004), showed that, unlike in xanthorhodopsin, in this system there is no energy transfer from bacterioruberin to retinal

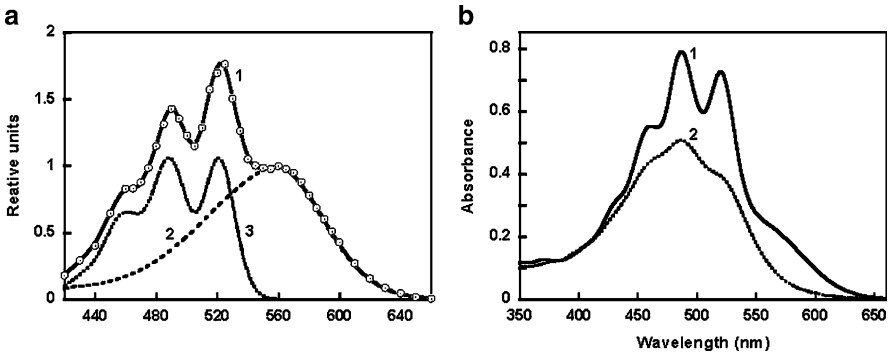

Fig. 17.3 (**a**) Action spectrum (1) of photoinhibition of respiration in *Salinibacter ruber* cells and its retinal (2) and carotenoid (3) components. Light absorbed by the carotenoid decreases the rate of cell respiration (as a result of back pressure from the light-induced electrochemical proton gradient), indicating its involvement in collecting energy for the transport process. From Boichenko et al. (2006). (**b**) Absorption spectra of fractions of *Salinibacter ruber* cell membrane containing: 1, xanthorhodopsin with bound salinixanthin; 2, salinixanthin not bound to xanthorhodopsin

(Boichenko et al. 2006). This finding emphasizes the uniqueness of proteins like xanthorhodopsin, and implies that antenna function utilizing excitation energy transfer did not emerge among the archaea but appeared later during evolution. The function of bacterioruberin in archaeal membranes must be primarily photoprotection and structural stability (Yoshimura and Kouyama 2008), whereas salinixanthin has a clear energetic role, perhaps in addition to the two others.

17.3 Spectroscopic Evidence for a Specific Binding Site for Salinixanthin and Its Interaction with Retinal

The cell membrane of *Salinibacter ruber* after dialysis was separated into two fractions (Balashov et al. 2005); the lighter fraction in the supernatant was characterized by an absorption spectrum with a maximum at 488 nm and poorly resolved shoulders on both sides. It contained salinixanthin which accounts for >95% of all carotenoids with a small amount of β-carotene also present (Lutnaes et al. 2002). The heavier fraction in the pellet exhibited sharp, well resolved bands at 522, 486 and 456 nm from the salinixanthin bound to xanthorhodopsin and a broad retinal band with maximum at ca. 560 nm (Fig. 17.3b), bands similar to those in the action spectrum.

Evidence for specific and rigid binding of salinixanthin in xanthorhodopsin is from experiments in which the retinal chromophore was removed and then reconstituted with all-*trans* retinal (Balashov et al. 2005, 2006). Incubation with hydroxylamine results in cleavage of the C=N bond that connects the retinal to the protein and elimination of the 560 nm retinal chromophore band, which shifts to

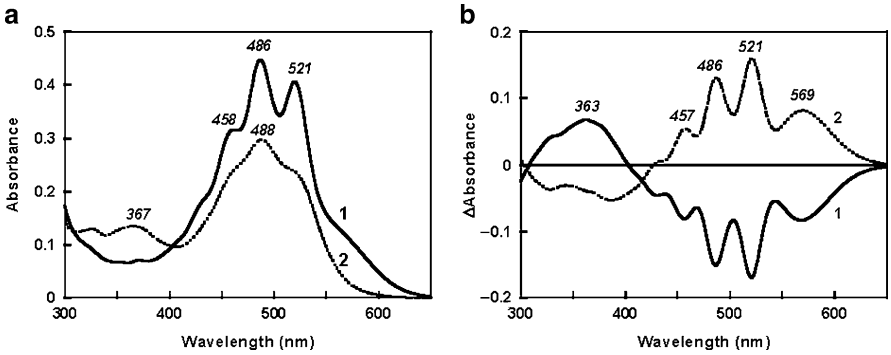

Fig. 17.4 (**a**) Absorption spectra of: 1, membranes containing xanthorhodopsin; 2, after incubation with 0.2 M hydroxylamine during illumination (to hydrolyze the C=N bond and remove retinal from the binding site). (**b**) Absorption changes accompanying: 1, hydrolysis of the Schiff base with hydroxylamine (curve 2 minus 1 in panel (**a**)); 2, reconstitution of xanthorhodopsin with all trans retinal. Adapted from Imasheva et al. (2008)

362 nm upon formation of the retinal oxime (Fig. 17.4). This is typical for retinal proteins. Surprisingly, the carotenoid bands are also strongly affected (spectra 1 and 2 in Fig. 17.4a and the difference spectrum 1 in Fig. 17.4b). They become less intense and broader than in untreated xanthorhodopsin. Addition of retinal after treatment with hydroxylamine results in the re-formation of the C=N bond and the reappearance of retinal protein band, accompanied by reversal of the changes in the absorption spectrum of the carotenoid (spectrum 2 in Fig. 17.4b): the vibronic bands become narrower and more intense as in the untreated protein. The structured spectrum was attributed to decreased conformational heterogeneity of the carotenoid because of restriction of the rotation of its ring around the C6–C7 bond by the retinal protein (Balashov et al. 2006); such rotations and conformational heterogeneity are typical for similar compounds with conjugated rings (Christensen and Kohler 1973; Buchecker and Noack 1995). The conjugated keto group is known to eliminate the vibronic structure of carotenoid spectra (Britton 1995), but it can be at least partially recovered in nonpolar solvents where interaction with carboxyl oxygen are minimized, and in frozen solvents where intramolecular motions are reduced (Ke et al. 1970).

The restoration of the well resolved structure of the carotenoid spectrum by insertion of the retinal into its binding site occurs before (and even in the absence of) formation of the protonated Schiff base, as experiments with retinal analogs indicate (Imasheva et al. 2008). In reconstitution experiments, the 13-desmethyl retinal analogue as well as the analogue with a "locked" C13=C14 bond, forms the protonated Schiff base linkage much more slowly than retinal (Imasheva et al. 2008). This provided the opportunity to observe carotenoid changes at various stages of retinal binding. When immobilization of the salinixanthin keto ring is followed by measuring the development of its highly structured bands, it is found to occur earlier than the appearance of the 560 nm band of the protonated Schiff base as retinal analogues with slower reconstitution rates are used. Thus, the carotenoid

is "re-bound" (assumes its twisted and immobilized conformation) in its specific site even before the covalent bond to a lysine via a Schiff base is formed (Imasheva et al. 2008; Smolensky and Sheves 2009).This implicates the retinal chain and ionone ring in the interaction with the carotenoid, as was recently confirmed by X-ray crystal structure (Luecke et al. 2008), see below. When reconstitution is with retinol, which cannot form a Schiff base, the carotenoid exhibits spectral changes similar to those when retinal is added. This provides further evidence that restriction of conformational heterogeneity of the carotenoid is through steric interaction with the retinal, as the retinal enters the binding site.

Salinixanthin in an organic solvent does not exhibit optical activity in the visible (a Cotton effect), but when bound it becomes chiral, as detected by circular dichroism (CD) (Balashov et al. 2006). Thus, the native xanthorhodopsin complex has an asymmetric conformation. Like the structured absorption spectrum, the bands of the CD spectrum are controlled by the retinal. Hydrolysis of the retinal Schiff base with hydroxylamine and the ensuing removal of retinal from the binding site abolish optical activity (Balashov et al. 2006). This shows that in the native state the retinal is responsible for forcing the antenna into an asymmetric conformation. Analogies with other carotenoids (Buchecker and Noack 1995) suggest that this involves a turn of its ring moiety (Balashov et al. 2006). Part of the CD spectrum is likely to be from electronic interactions of the conjugated systems in the two chromophores, as in the light harvesting complexes of photosynthetic bacteria (Georgakopoulou et al. 2004).

Independent evidence for close interaction of the carotenoid antenna with the retinal chromophore was obtained in studies of spectral changes that accompany the photocycle reactions. Formation of the K intermediate causes a small (1–2 nm) blue shift of the carotenoid spectrum (Balashov et al. 2005) which might originate from changes in either electrostatic field or steric interaction with the ionone ring of retinal (see below). At a later time in the cycle, the carotenoid exhibits a different type of transient change, which can be described as a broadening of the spectrum from increased freedom for bond rotations, i.e., loosening of the binding site (Balashov et al. 2005).

The carotenoid antenna can be selectively oxidized with ammonium persulfate with relatively little effect on the retinal absorption spectrum and photocycle kinetics. The latter exhibits only a small decrease in the photocycle turn-on (Imasheva et al. 2011).

17.4 Xanthorhodopsin as a Proteorhodopsin Homologue: Similarities in the pK_a of the Counterion and the Photocycle

Proton pumps depend on the reversible protonation and deprotonation of groups inside the protein and at its surface, and thus their proton affinities are of interest, especially that of the counterion to the protonated retinal Schiff base. The pK_a of the

counterion of xanthorhodopsin is lower value in detergent (Imasheva et al. 2006), more like that in proteorhodopsin, pK_a 7.5 (Dioumaev et al. 2003; Imasheva et al. 2004) than in bacteriorhodopsin, pK_a 2.6 (Balashov et al. 1996) or archaerhodopsin, pK_a 3.5 (Ming et al. 2006). In the latter microbial retinal proteins the pK_a of the counterion can be easily determined by a large (30–40 nm) red shift of retinal absorption band at low pH. Surprisingly, in xanthorhodopsin there is only a small (3 nm) red shift between pH 2 and 12 (Imasheva et al. 2006). A similarly small shift was observed for the highly homologous *Gloeobacter* rhodopsin (Miranda et al. 2009). The pH dependence of the yield of the M photointermediate, another indication of the counterion protonation (because one of the aspartate groups in the counterion, Asp85 in bacteriorhodopsin serves as a proton acceptor during the photocycle), yields the same pK_a. This provides independent evidence that the pK_a of the counterion in xanthorhodopsin is 6.0 in detergent (Imasheva et al. 2006). In bacteriorhodopsin, the counterion is a pair of aspartates (Asp85 and Asp212). The unusually small spectral shift in xanthorhodopsin indicates that the counterion in this protein might have a different structure. This was confirmed by the crystallographic structure. It showed rotation and close interaction of Asp96 (homologous to Asp85 in bacteriorhodopsin) with a histidine and presence of only single water at the active site, corresponding to Wat402 in bacteriorhodopsin. The high pK_a makes xanthorhodopsin a proteorhodopsin-like proton pump, different from bacteriorhodopsin. Mutagenesis of proteorhodopsin indicated that the aspartate serving as a counterion to the Schiff base interacts with histidine in this protein also (Bergo et al. 2009). Unlike the archaeal rhodopsins, the eubacterial rhodopsins do not function at neutral or acid pH, because the counterion will not function as proton acceptor below its pK_a (Dioumaev et al. 2003).

Studies of the pH dependence of the recovery of the initial state in the photocycle of xanthorhodopsin reveal two pK_a's, 6.0 and 9.3. The changes with pK_a 6 reflect the two kinds of photocycles, at acidic and alkaline pH. They originate from the protonation state of the counterion (presumably Asp96, or probably the Asp96–His62 pair, see below). The second pK_a, at 9.3, has been attributed to the pK_a of the acidic group (Glu107) that is the internal proton donor to the deprotonated retinal Schiff base in the M intermediate (Imasheva et al. 2006). It is 2 pH units higher than in bacteriorhodopsin (Balashov 2000).

Overall, the photocycle of xanthorhodopsin exhibits features more similar to those of proteorhodopsin than bacteriorhodopsin, with proton uptake occurring first, followed by release coincident with the last step at the end of the photocycle. The sequence of reactions includes formation of the K, L, M, N and O like intermediates. The kinetics at pH 8.8 can be fit with six exponentials (7.5 μs, 35 μs, 280 μs, 1.3 ms, 10 ms and 100 ms) (Balashov et al. 2005). The K to L reaction is slower, and occurs at a higher cryogenic temperature than in bacteriorhodopsin, >175 K versus 130 K (Litvin et al. 1975; Lozier et al. 1975; Balashov et al. 2005). That helped to establish the evolution of the primary photoproduct K as at least two subsequent states, XR $\leftrightarrow$ K_0 $\rightarrow$ K_E, where K_0 is observed almost as a pure species at 80 K and undergoes transition to K_E between 80 and 180 K (Dioumaev et al. 2010). The two K forms are analogous to those in bacteriorhodopsin

(Rothschild et al. 1985; Maeda et al. 2004). They differ substantially in their HOOPs bands and water bands and most likely represent untwisting and relaxation in the strained 13-cis retinal chromophore after its photoisomerization from the initial all-trans in the XR $\rightarrow$ K_0 photoreaction.

Illumination of xanthorhodopsin at low pH (pH 3) results in formation of long-lived photoproducts (Imasheva et al. 2006) similar to the 13-*cis*-states observed in proteorhodopsin (Imasheva et al. 2004, 2005). Remarkably, the spectral bands of the antenna carotenoid are greatly affected in these states (showing broadening and decrease in the maximum amplitude), indicating a connection between the isomeric state of the retinal chromophore and the carotenoid binding.

17.5 Excited States and Fluorescence of the Retinal and the Salinixanthin Chromophores of Xanthorhodopsin: Efficiency and Pathway of Energy Transfer

Direct evidence for excitation energy transfer from the carotenoid to the retinal was obtained by detecting fluorescence of the retinal chromophore induced by quanta absorbed by the carotenoid (Balashov et al. 2008). It eliminated alternative interpretations of the action spectra, e.g., that the carotenoid is involved in proton transfer through an unknown mechanism, or regulates in some manner the functioning of retinal but without supplying the energy for the pump. Fluorescence of the retinal can be detected from its strongly allowed $1B_u^+$ excited state (using the C_{2h} symmetry group notation), which in retinal proteins with protonated Schiff bases is the lowest excited state, the S_1 state (Birge 1990). The retinal fluorescence is weak (quantum yield ca. 2–5 $\times$ 10^{-4}, depending on pH) but the emission from the carotenoid is tenfold weaker (see below). The presence of the carotenoid bands in the excitation spectrum for the retinal emission at 720 nm (Fig. 17.5) provided the final evidence for excited-state energy transfer (Balashov et al. 2008; Lanyi and Balashov 2008).

The excitation spectrum for the retinal emission, sampled at 720 nm, is similar to the excitation spectrum obtained earlier for the physiological responses (Fig. 17.2), i.e., light-induced proton transport and photoinhibition of respiration (Balashov et al. 2005; Boichenko et al. 2006). From the comparison of the relative amplitude of the carotenoid bands in the excitation and absorption spectra (Fig. 17.5a, spectra 1 and 2), and taking into account a small contribution from the carotenoid fluorescence (see below), the efficiency of energy transfer from salinixanthin to the retinal was estimated to be 45 $\pm$ 5% (Balashov et al. 2008). This was determined without using extinction coefficients for the two chromophores. The earlier lower estimate at 33% (Boichenko et al. 2006) was obtained with the assumption that the extinction of the carotenoid is ca. threefold larger than that of the retinal chromophores. This appears to be an overestimate: a more accurate ratio is about 2.5, in the range of 130,000–150,000 L/(mol cm) (Balashov et al. 2008).

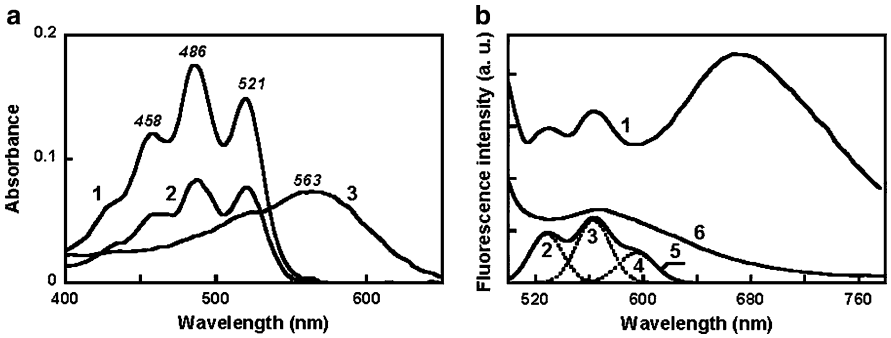

Fig. 17.5 (**a**) Components of the excitation and absorption spectra of xanthorhodopsin, pH 5.5: 1, carotenoid component in the absorption spectrum; 2, carotenoid component in the excitation spectrum; 3, retinal component in the absorption and excitation spectra. (**b**) 1, fluorescence spectrum of xanthorhodopsin upon excitation at 470 nm. The bands at 529 and 565 nm are from salinixanthin emission. A broader band with maximum at 690 nm belongs to retinal fluorescence; 2, 3 and 4, Gaussian fits (components) of the salinixanthin emission from the S_2 excited state; 5, their sum, approximating the short wavelength part of bound salinixanthin emission spectrum; 6, same as 1, but after hydrolysis of the Schiff base with hydroxylamine. Both retinal component and sharp bands of bound salinixanthin are missing from this spectrum. After Balashov et al. (2008)

The contribution of carotenoid emission to the total emission at 720 nm (where the retinal emission was sampled) is small, as indicated by the good agreement of the "physiological" action spectrum and the fluorescence excitation spectrum. Nevertheless, an estimate of the contribution from the fluorescence spectrum of carotenoid was necessary. Detection of this emission was crucial also for determining the mechanism and pathway of the energy transfer. Fluorescence of carotenoids with long conjugated chains has been detected before, but only from solutions of carotenoids in organic solvents. It occurs from a $^1B_u^+$ – like state (S_2), and is extremely weak (reviewed in (Frank and Cogdell 1993; Polívka and Sundström 2004)).

In the xanthorhodopsin fluorescence spectrum, three sharp bands (different from the retinal bands and the background signal) at 529, 565 and 595–605 nm were identified as the carotenoid emission (Balashov et al. 2008). These bands (shown in Fig. 17.5b) exhibit the features peculiar to the fluorescence from the S_2 excited state of carotenoids with long conjugated chains studied in organic solvents: very low quantum yield (4×10^{-5}), small Stokes shift (ca. 300 cm^{-1}), and an approximate mirror-image symmetry of the absorption and fluorescence spectra. The contribution of carotenoid emission to the total emission at 720 nm is less than 5%. The quantum yield corresponds to a very short (ca. 70 fs) lifetime for the excited state of bound carotenoid (Balashov et al. 2008), a value confirmed by direct time resolved experiment following the decay of the absorption band associated with the S_2 to S_n transition (Polívka et al. 2009).

The energy transfer occurs from the S_2 excited state of the carotenoid to the S_1 state of the retinal. The intense absorption bands of carotenoids are from electron transitions from the ground S_o to the S_2 excited state. Transition from S_o to the S_1 state is forbidden but the latter state is populated in internal conversion from S_2.

In the light-harvesting complexes of green plants and photosynthetic bacteria, the carotenoid to chlorophyll energy transfer occurs from both the S_2 and S_1 excited state levels of a carotenoid (Polívka and Sundström 2004). The S_1 level of salinixanthin is estimated to be in the near IR region, between 750 and 850 nm (Balashov et al. 2008). Thus, in xanthorhodopsin, the carotenoid S_1 level cannot serve as a donor because it is below the S_1 level of the retinal at 560 nm. Energy transfer must occur mostly from the S_2 excited state level of salinixanthin to the S_1 level of retinal (Balashov et al. 2005).

This prediction is confirmed in experiments with sodium borohydride (Balashov et al. 2008). Reduction of the double C=N bond of the retinal Schiff base to a single bond shifts the absorption of retinal from 560 to 360 nm, with no (or almost no) effect on the carotenoid absorption bands because retinal remains in the binding site. The large blue shift of the retinal band upon reduction eliminates any possibility of energy transfer since its energy level becomes much higher than that of the carotenoid. Under these conditions there is a twofold increase in the intensity of the carotenoid emission at 529 and 565 nm, characteristic of the S_2 level (Balashov et al. 2008). This provides evidence that the S_2 level is the only (or the major) source of energy for the S_1 state of retinal chromophores, the lowest resolved singlet excited state (Birge and Zhang 1990).

Measurements of the spectral changes in the excited state and their dynamics on the femtosecond time scale confirm and extend the conclusions from steady-state spectroscopy (Polívka et al. 2009). Here also, borohydride treatment, which reduces the retinal Schiff base $C{=}NH^+$ from double to single bond and shifts the absorption maximum far to the blue but unlike the hydroxylamine treatment retains the retinal in its binding site, affords suitable comparison of the system with and without energy transfer. The more rapid decay of the S_2 state of salinixanthin when the retinal chromophore is available as energy acceptor, 66 fs versus 110 fs, reveals the presence of the expected additional decay channel, and yields an efficiency of ca. 40% for the energy transfer (Polívka et al. 2009). No change in the decay of the carotenoid S_1 state is found (ca. 3 ps), consistent with the expectation that its level is below the S_1 state of the retinal (scheme in Fig. 17.6). These results are supported by a recent independent femtosecond study (Zhu et al. 2010).

The rate constant for the Förster resonance energy transfer is proportional to the spectral overlap integral of carotenoid emission and retinal absorption and the square of the coloumbic interaction (electronic coupling) of the two chromophores, V (Scholes 2003). From the spectral and kinetic data the latter was estimated to be in the range of 160–210 cm^{-1} (Polívka et al. 2009), a value comparable with those in carotenoid-bacteriochlorophyll antenna systems (Krueger et al. 1998). Theoretical calculations based on the crystal structure of xanthorhodopsin, that took into account the mutual geometry of the chromophores yielded a similar estimate (Fujimoto and Hayashi 2009).

The S_2 state of salinixanthin being very short-lived, the efficient energy transfer requires close proximity of the donor to the acceptor. The efficiency of the excitation energy transfer depends on the overlap integral of the donor fluorescence and acceptor absorption and their distance. The fluorescence from the S_2 level of

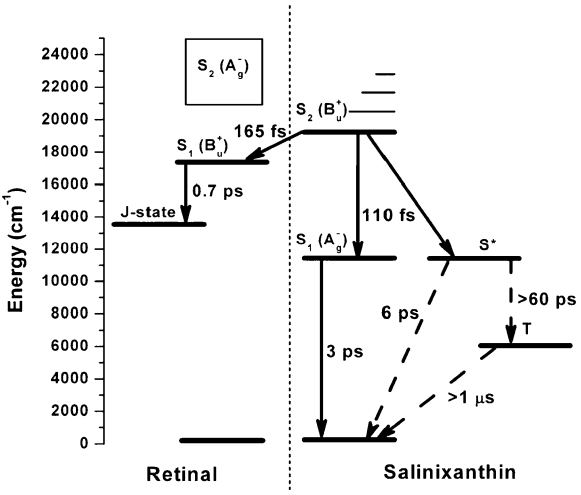

Fig. 17.6 Scheme of excited states of the retinal and the carotenoid chromophores of xanthorhodopsin, the energy transfer pathway from the S_2 of the carotenoid to S_1 of retinal and alternative relaxation processes as inferred from femtosecond time resolved absorption changes (Polívka et al. 2009). Numbers by the *arrows* are time constants for the pathways of energy conversion in xanthorhodopsin (pH 8). S* is a substrate of the S_1 state. T is a triplet state. The lifetime of the S_2 state is 66 fs (sum of the two processes with time constants 110 and 165 fs). *Dotted vertical line* separates the excited states of the retinal chromophore (to the *left*) and salinixanthin antennae (to the *right*). From Polívka et al. (2009)

carotenoid, with maxima at 529 nm and 565 nm, optimally overlaps with the retinal absorption with a maximum at 560 nm. Calculations using the Förster equation for the efficiency of energy transfer and the experimentally obtained values for overlap integrals and quantum yield of carotenoid S_2 fluorescence yielded the distance between the centers of the carotenoid polyene chain and the retinal as ca. 11 Å (Balashov et al. 2008). This is a very rough estimate only, because the dimensions of the two linear chromophores are comparable to this distance, a case that is not described accurately by the original Förster equation.

The contribution of the salinixanthin bands to the excitation spectrum of the retinal chromophore fluorescence strongly depends on the polarization of the excitation and emission beams (Balashov et al. 2008). This means that there is a substantial angle ($\gg 0^o$) between the transition moments of the $S_0 \rightarrow S_2$ carotenoid absorption and $S_1 \rightarrow S_0$ retinal fluorescence. From measurement of the excitation anisotropy the angle was determined to be $56 \pm 3°$ (Balashov et al. 2008), near the 46° angle between the geometric axes of the two conjugated chains (Fig. 17.7a) determined later by X-ray diffraction (Luecke et al. 2008). The discrepancy is most likely because of an off-axis orientation of the transition moment, as in rhodopin (Georgakopoulou et al. 2003). The angle appears to be a compromise between the best efficiency for energy transfer (parallel) and the ability to collect incident light by the dual chromophore system at all angles of polarization (perpendicular). In bacteriorhodopsin the retinal is tilted 21° from the

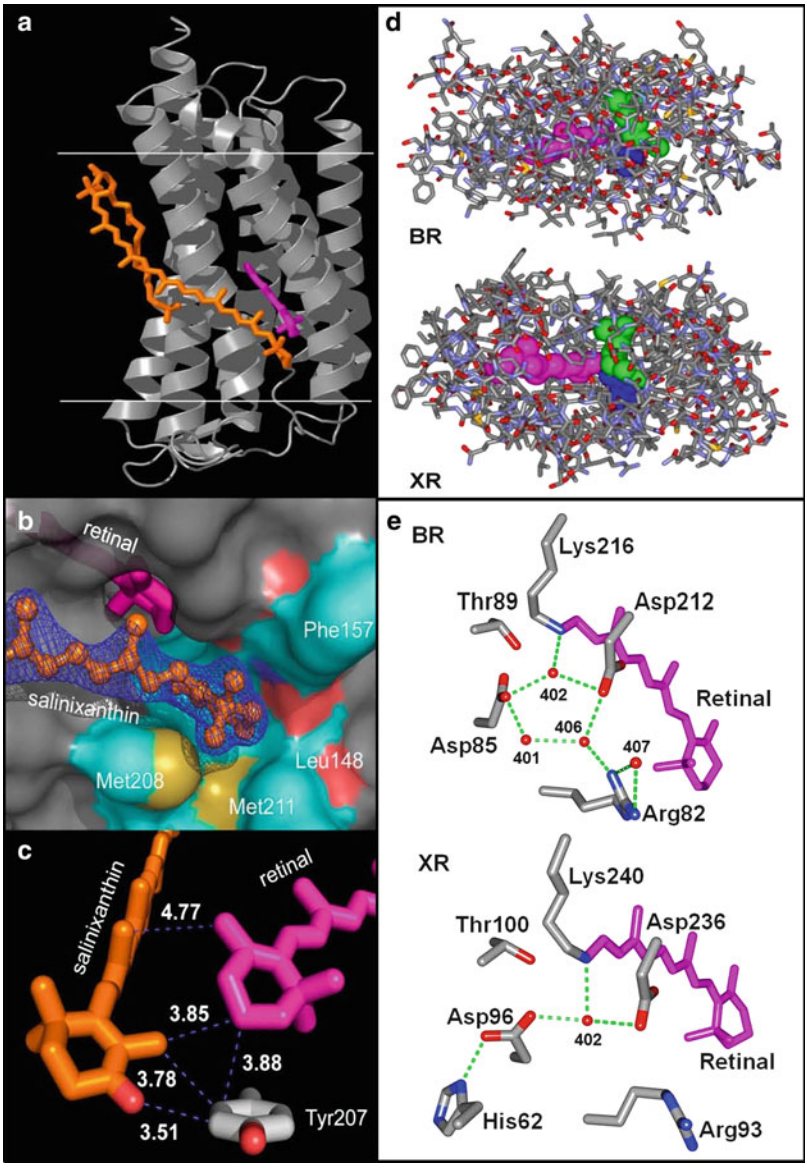

Fig. 17.7 *Left panel*. Location of salinixanthin (*orange*) and retinal (*magenta*) in the X-ray structure of xanthorhodopsin. (**a**) The extended carotenoid is tightly bound on the surface of xanthorhodopsin. The angle between the chromophore axes is 46°. *Horizontal lines* indicate the approximate boundaries of the lipid bilayer. (**b**) The binding pocket of the salinixanthin keto ring is formed by Leu148, Gly156, Phe157, Thr160, Met208, and Met211, as well as the retinal β-ionone ring. (**c**) The keto ring of the carotene is rotated 82° out of plane of the salinixanthin-conjugated system and is in van der Waals distance of the retinal β-ionone and the phenolic side chain of Tyr207. From Luecke et al. (2008). *Right panel*. Comparison of bacteriorhodopsin and xanthorhodopsin. (**d**) A view on bacteriorhodopsin and xanthorhodopsin from the extracellular side showing a cleft extended to the

membrane plane. The high degree of homology of residues in the retinal binding sites of the two proteins suggests that the retinal will be oriented similarly in xanthorhodopsin. In this case, the carotenoid will be tilted either 13° or 55° to the membrane normal, and the structure of the protein (Luecke et al. 2008) indicates that the latter is the case. The tilt ensures that all but the glycoside moiety of the long and roughly linear carotenoid is immersed in the hydrophobic region of the membrane.

17.6 Crystal Structure of Xanthorhodopsin on Carotenoid Binding Site and Novel Features of the Eubacterial Proton Pump

In the crystal structure (Luecke et al. 2008) the carotenoid is seen to be buried at the protein–lipid boundary, and lies transverse against the outer surface of helix F at a 56° angle to the membrane normal (Fig. 17.7a). Its keto ring contacts residues at the extracellular ends of helices E and F and the β-ionone ring of the retinal, and is rotated 82° from the plane of the methyl group of its polyene chain and therefore from the plane of the extended π-system (Fig. 17.7b). The keto group oxygen is not hydrogen-bonded. Immobilization of the ring and its acutely out-of-plane orientation minimizes participation of its two double bonds in the conjugated π-system, and explains the well-resolved vibronic bands of the bound carotenoid, the lack of a red-shift of the bands relative to the bands in organic solvents, and the strong CD bands in the visible region. The dependence of the carotenoid spectrum on the retinal is explained by the fact that the retinal β-ionone ring is part of the carotenoid binding site. The relatively rigid polyene chain is wedged in a slot on the outside of helix F, with one side formed by the Leu194 and Leu197 side-chains and the other by the Ile205 side-chain. The carotenoid glucoside is hydrogen-bonded to the C=O and the NH_2 of the amide side-chain of Asn191, as well as NH1 of Arg184.

The keto ring of the carotenoid is in the space occupied by Trp-138 in bacteriorhodopsin, whose bulky side-chain fixes the position of the retinal ionone ring in that protein. In xanthorhodopsin it is replaced by a glycine, whose smaller volume makes room for the carotenoid. Another difference is Glu141 of xanthorhodopsin, which is an alanine in bacteriorhodopsin but a conserved glutamate in proteorhodopsins involved in spectral tuning (Kralj et al. 2008).

The center-to-center distance of the two chromophores is 11.7 Å, i.e., about the same as the 11 Å estimate. The two polyenes may interact more intimately than this distance predicts, however, because the retinal β-ionone ring is within van der Waals distance of the carotenoid keto ring (Fig. 17.7c). Both rings are in contact

Fig. 17.7 (continued) retinal in xanthorhodopsin. Retinal is in pink, Arg82 and its homolog is in blue and Asp212 is in green. (**e**) Active site structure in bacteriorhodopsin and xanthorhodopsin based on high resolution crystal structures, 1.55 Å for bacteriorhodopsin, 1C3W, (Luecke et al. 1999b) and 1.9 Å for xanthorhodopsin, 3DLL (Luecke et al. 2008)

with the aromatic ring of Tyr207 between them. This is unlike the crystal structure of archaerhodopsin (Yoshimura and Kouyama 2008), the other proton pump that contains a carotenoid, bacterioruberin, but without antenna function, where the corresponding inter-chromophore center-to-center distance is 17 Å, and the closest approach of bacterioruberin to the retinal at 12 Å. Energy transfer in that protein is obviously excluded by the large distance between the chromophores.

Solving the X-ray structure of xanthorhodopsin defined not only the geometry of carotenoid-retinal interaction, but provided also better understanding of the broader question of the transport mechanism in microbial light-driven proton pumps. Until now, a crystal structure was not available for any of the numerous proteorhodopsins, but at this stage, because they share many common features with xanthorhodopsin, the new structure may be considered as a model for eubacterial rhodopsins in general. The structure helped to improve the initial sequence alignment of xanthorhodopsin and proteorhodopsin (Balashov et al. 2005), and points to an even large homology with the latter (Fig. 17.1b).

Remarkably, in the 1.9-Å resolution structure of xanthorhodopsin there are great differences from the disposition of the main-chain of bacteriorhodopsin (Fig. 17.7a). Helices A and G are longer by four and nine residues, respectively, and their tilt and rotation, particularly of helix A, are considerably different. The 28 residues that comprise helix B are four residues shifted in the sequence toward the C terminus (i.e., toward the extracellular side). In bacteriorhodopsin, the interhelical B–C antiparallel β-sheet interacts with the D–E loop, while in xanthorhodopsin it reorients dramatically to interact with the Arg8 peptide C=O near the N terminus, where it forms a three-stranded β-sheet. As a result, the B–C loop is displaced, by as much as 30 Å, toward the periphery of the protein. This uncovers a large cleft at the extracellular surface that extends far into the interior and brings the aqueous interface near to functional residues that are buried in bacteriorhodopsin (Fig. 17.7d). The absence of a hydrogen-bonded network of polar groups and water in this region correlates with the observed lack of proton release to the extracellular surface upon deprotonation of the retinal Schiff base in the photocycle (Luecke et al. 2008; our unpublished results).

In bacteriorhodopsin, Wat402 receives a hydrogen-bond from the protonated retinal Schiff base and donates hydrogen-bonds to the two anionic residues, Asp85 and Asp212 (Luecke et al. 1998). This arrangement is conserved in xanthorhodopsin. However, the extracellular hydrogen-bonded aqueous network is missing entirely (Fig. 17.7e), and the single glutamate is far removed from Arg93, the homologue of Arg82 in bacteriorhodopsin (>18 Å vs. 7.3 Å in bacteriorhodopsin). Rearrangement of the Arg93 side-chain is unlikely to occur in the xanthorhodopsin photocycle, because its NH1 and NH2 are both hydrogen-bonded to the peptide carbonyl of Gln229 instead of water molecules. In bacteriorhodopsin, a pair of glutamate residues, Glu194 and Glu204 (Brown et al. 1995; Balashov et al. 1997), coordinates a hydrogen-bonded water network from which a proton is released to the extracellular surface (Garczarek et al. 2005) after the retinal Schiff base is deprotonated and the counterion is protonated in M intermediate and the side-chain of Arg-82 moves toward the glutamate pair (Luecke et al. 1999a). As

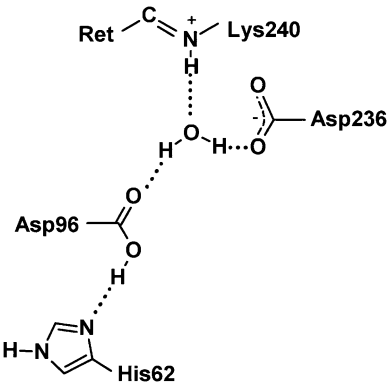

Fig. 17.8 Asp-His counterion to the Schiff base of xanthorhodopsin. The Schiff base interacts with the counterion through a water molecule (Wat402). After Luecke et al. (2008)

xanthorhodopsin, the other eubacterial pumps also contain only one of these carboxylic acid residues, homologous to Glu194 of bacteriorhodopsin.

One of the distinguishing features of eubacterial proton pumps is that the pK_a of the primary proton acceptor is not as low as 2.6 in bacteriorhodopsin, but near 6–7 (see above). The origin of the increased proton affinity had been an unsolved problem. In xanthorhodopsin, ND1 of His62 is hydrogen-bonded to OD1 of Asp96 (Figs. 17.7e and 17.8). With a length of 2.4–2.5 Å, this is a very short hydrogen-bond that suggests that the proton is strongly shared by the imidazole ring and the carboxylate. The aspartate–histidine complex, with an expected pK_a higher than the aspartate alone, must be thus regarded as the Schiff base counterion. The archaeal rhodopsins do not contain this histidine. If otherwise the analogy with bacteriorhodopsin holds, it is the anionic, rather than the neutral complex, that is the proton acceptor of the Schiff base in the photocycle.

A histidine at this position is highly conserved in the proteorhodopsins, making it likely that the aspartate–histidine complex is a general characteristic of eubacterial pumps. Once protonated in the photocycle, the His62–Asp96 complex would be a good candidate for the origin of the proton released to the medium upon deprotonation of the retinal Schiff base, but at neutral pH, at least, such early proton release does not occur (Luecke et al. 2008). Asp–His pairs connected with a strong short hydrogen bond are involved in catalysis of different reactions in many enzymes, such as α-chymotrypsin (Cleland et al. 1998).

In the cytoplasmic region of bacteriorhodopsin, the proton donor Asp96 is in an anhydrous environment that constitutes the hydrophobic barrier in the cytoplasmic half of the protein (Belrhali et al. 1999; Luecke et al. 1999b). This, and the fact that it donates a hydrogen-bond to OD1 of Thr46, raises its pK_a. The aspartic acid becomes a proton donor to the Schiff base during the photocycle only after hydration of this region that includes a hydrogen-bonded chain of four water molecules to connect the proton donor to its acceptor (Schobert et al. 2003). In xanthorhodopsin, as in the proteorhodopsins, these residues are replaced by a glutamic acid and a serine. The carboxyl is hydrogen-bonded to Wat502 that connects to the peptide carbonyl of Lys240. It appears therefore, that in xanthorhodopsin part of the

cytoplasmic hydrogen-bonded chain of water molecules between the retinal and the proton donor is in position favorable for proton transport already in the initial state, which might explain accelerated reprotonation of the Schiff base in the photocycle.

17.7 Other Retinal Proteins with Light-Harvesting Antennae: Reconstitution of Gloeobacter Rhodopsin with Salinixanthin and Echinenone

The X-ray structure of xanthorhodopsin reveals that the 4-keto ring is in the space created by replacement of the bulky Trp138 of bacteriorhodopsin with a Gly in xanthorhodopsin. This gave the clue for a search of other retinal proteins that might contain an antenna similar to salinixanthin. Over a dozen of sequences of retinal proteins, presumably pumps and sensors, from various groups (*Alphaproteobacteria, Actinobacteria, Cyanobacteria, Flavobacteria* and others), especially in xanthorhodopsin clade, have Gly instead of Trp at this site (Table 17.1). To

Table 17.1 Representative list of organisms harboring genes homologous to xanthorhodopsin of *Salinibacter ruber*

Species carrying gene homologous to XR	Accession number[a]	Homology to XR (%)	Key homologous residues[b]
Salinibacter ruber DSM 13855	YP_445623	100	H D E G
Gloeobacter violaceus PCC 7421	NP_923144	53	H D E G
Thermus aquaticus Y51MC23 ctg62	ZP_03495873	53	H D E G
Roseiflexus sp. RS-1	YP_001277280	52	H D E G
Methylophilales bacterium HTCC2181	ZP_01551538	49	H D E W
Alphaproteobacterium BAL199	EDP63929	48	H D E G
Octadecabacter antarcticus 238	ZP_05063020	47	H D E G
Actinobacterium MWH-EgelM2-3.D6	ACN42852	46	H D E G
"*Candidatus* Aquiluna rubra"	ACN42850.1	45	H D E G
Fulvimarina pelagi HTCC2506	ZP_01440547	34	S N Q G
Geodermatophilus obscurus DSM 43160	ZP_03889903	32	A D E G
Kineococcus radiotolerans SRS30216	EAM73404	32	S D E G
Exiguobacterium sp. AT1b	YP_002885111	31	H D K G
Polaribacter sp. MED152	ZP_05108337	32	H D E G
Dokdonia donghaensis MED134	EAQ40507	31	H D E G
Polaribacter irgensii 23-P	ZP_01117885	31	H D E G
Flavobacteria bacterium BAL38	ZP_01734914	29	H D E G
Psychroflexus torquis ATCC 700755	ZP_01253360	29	H D E G

[a]Protein sequence accession numbers obtained from NCBI using BLASTP

[b]Four residues homologous to H62, D96 (proton acceptor), E108 (proton donor) and G178 of xanthorhodopsin. All sequences shown in the table except one contain glycine homologous to Gly178 of xanthorhodopsin, which makes these proteins potential candidates for binding of a carotenoid antenna with a keto ring similar to that in salinixanthin as shown for gloeobacter rhodopsin (Imasheva et al. 2009)

test that at least some of them are indeed capable of binding carotenoid antenna, we "implanted" (reconstituted) salinixanthin into gloeobacter rhodopsin expressed in *E. coli*, and showed that it transfers energy to the retinal chromophore (Imasheva et al. 2009). Replacing the Gly with a Trp abolishes carotenoid binding, thus confirming that accommodation of the ring is crucial for the antenna binding. Surprisingly, minor modification of salinixanthin that involves reduction of its 4-keto C=O group to C–OH also practically eliminates binding and energy transfer in both *Gloeobacter* rhodopsin (Balashov et al. 2010) and xanthorhodopsin (Imasheva et al. 2011). This suggests the importance of the 4-keto group in the carotenoid binding and energy transfer. This conclusion was supported by the experiments with β-carotene and echinenone (Balashov et al. 2010). The host organism, *Gloeobacter violaceus*, does not contain salinixanthin, but a simpler carotenoid, echinenone, also with a 4-keto ring but lacking glucoside and acyl tale, is present in addition to β-carotene and oscillol. We found that while β-carotene does not bind, its 4-keto derivative, echinenone, does, as follows from the characteristic changes in the absorption and CD spectra and fluorescence excitation spectrum which shows echinenone bands in addition to the retinal band (Balashov et al. 2010). This result again points to the 4-keto group as a key factor in the binding of carotenoids in these proteins. Reconstitution with echinenone is slower than with salinixanthin, apparently from lack of the 2′ hydroxy group and the acyl glycoside.

17.8 Conclusions

Despite the short history of xanthorhodopsin research, it has uncovered new features not seen before in light-driven retinal based pumps. This includes the existence of a light-harvesting carotenoid antenna, and a structure for the proton translocating pathways dramatically different from those in bacteriorhodopsin. Genetic homology with many members of xanthorhodopsin clade and proteorhodopsins suggest that these features might be common to other numerous eubacterial pumps and represent a considerable variation of a design of retinal-based proton pump as has been known from bacteriorhodopsin research.

Acknowledgments The authors would like to thank all collaborators involved in exploration of xanthorhodopsin, especially Prof. J Antón for bringing *S. ruber* to our attention and helpful advice, Profs. T Polívka and V Sundström and their colleagues for femtosecond experiments, Prof. H Luecke for refinement of xanthorhodopsin structure from X-ray diffraction data, Dr. B Schobert for crystallization of xanthorhodopsin, Dr. ES Imasheva for spectroscopic studies, purification, and help in preparation of the manuscript, JM Wang for isolation of *S. ruber* cell membranes and the late Dr. V Boichenko for action spectra in native cells. The research of xanthorhodopsin was supported in part by grants from the National Institutes of Health (GM29498), the Department of Energy (DEFG03-86ER13525) to JKL and the U.S. Army Research Office (W911NF-09-1-0243) to SPB.

References

Antón J, Oren A, Benlloch S, Rodríguez-Valera F, Amann R, Rosselló-Mora R (2002) *Salinibacter ruber* gen. nov., sp. nov., a novel, extremely halophilic member of the *Bacteria* from saltern crystallizer ponds. Int J Syst Evol Microbiol 52:485–491

Balashov SP (2000) Protonation reactions and their coupling in bacteriorhodopsin. Biochim Biophys Acta 1460:75–94

Balashov SP, Lanyi JK (2006) Bacteriorhodopsin. In: Rehn B (ed) Microbial biotechnology. Biological self-assembly systems and biopolymer-based nanostructures. Horizon Bioscience, Norfolk, pp 339–366

Balashov SP, Lanyi JK (2007) Xanthorhodopsin: proton pump with a carotenoid antenna. Cell Mol Life Sci 64:2323–2328

Balashov SP, Imasheva ES, Govindjee R, Ebrey TG (1996) Titration of aspartate-85 in bacteriorhodopsin: what it says about chromophore isomerization and proton release. Biophys J 70: 473–481

Balashov SP, Imasheva ES, Ebrey TG, Chen N, Menick DR, Crouch RK (1997) Glutamate-194 to cysteine mutation inhibits fast light-induced proton release in bacteriorhodopsin. Biochemistry 36:8671–8676

Balashov SP, Imasheva ES, Boichenko VA, Antón J, Wang JM, Lanyi JK (2005) Xanthorhodopsin: a proton pump with a light-harvesting carotenoid antenna. Science 309: 2061–2064

Balashov SP, Imasheva ES, Lanyi JK (2006) Induced chirality of the light-harvesting carotenoid salinixanthin and its interaction with the retinal of xanthorhodopsin. Biochemistry 45: 10998–11004

Balashov SP, Imasheva ES, Wang JM, Lanyi JK (2008) Excitation energy-transfer and the relative orientation of retinal and carotenoid in xanthorhodopsin. Biophys J 95:2402–2414

Balashov SP, Imasheva ES, Choi AR, Jung K-H, Liaaen-Jensen S, Lanyi JK (2010) Reconstitution of gloeobacter rhodopsin with echinenone: role of the 4-keto group. Biochemistry 49: 9792–9799

Béjà O, Aravind L, Koonin EV, Suzuki MT, Hadd A, Nguyen LP, Jovanovich SB, Gates CM, Feldman RA, Spudich JL, Spudich EN, DeLong EF (2000) Bacterial rhodopsin: evidence for a new type of phototrophy in the sea. Science 289:1902–1906

Béjà O, Spudich EN, Spudich JL, Leclerc M, DeLong EF (2001) Proteorhodopsin phototrophy in the ocean. Nature 411:786–789

Belrhali H, Nollert P, Royant A, Menzel C, Rosenbusch JP, Landau EM, Pebay-Peyroula E (1999) Protein, lipid and water organization in bacteriorhodopsin crystals: a molecular view of the purple membrane at 1.9 Å resolution. Structure 7:909–917

Bergo VB, Sineshchekov OA, Kralj JM, Partha R, Spudich EN, Rothschild KJ, Spudich JL (2009) His-75 in proteorhodopsin, a novel component in light-driven proton translocation by primary pumps. J Biol Chem 284:2836–2843

Birge RR (1990) Nature of the primary photochemical events in rhodopsin and bacteriorhodopsin. Biochim Biophys Acta 1016:293–327

Birge RR, Zhang C-F (1990) Two-proton double resonance spectroscopy of bacteriorhodopsin. Assignment of the electronic and dipolar properties of the low-lying $^1A_g^*$-like and $^1B_u^{*+}$-like π, π^* states. J Chem Phys 92:7178–7195

Boichenko VA, Wang JM, Antón J, Lanyi JK, Balashov SP (2006) Functions of carotenoids in xanthorhodopsin and archaerhodopsin, from action spectra of photoinhibition of cell respiration. Biochim Biophys Acta 1757:1649–1656

Britton G (1995) UV/Visible Spectroscopy. In: Britton G, Liaaen-Jensen S, Pfander H (eds) Carotenoids, vol 1B, Spectroscopy. Birkhäuser Verlag, Basel, pp 13–62

Britton G, Liaaen-Jensen S, Pfander H (2004) Carotenoids handbook. Birkhauser Verlag, Basel, Boston, Berlin

Brown LS, Jung K-H (2006) Bacteriorhodopsin-like proteins of eubacteria and fungi: the extent of conservation of the haloarchaeal proton-pumping mechanism. Photochem Photobiol Sci 5: 538–546

Brown LS, Sasaki J, Kandori H, Maeda A, Needleman R, Lanyi JK (1995) Glutamic acid 204 is the terminal proton release group at the extracellular surface of bacteriorhodopsin. J Biol Chem 270:27122–27126

Buchecker R, Noack K (1995) Circular dichroism. In: Britton G, Liaaen-Jensen S, Pfander H (eds) Carotenoids, vol 1B, Spectroscopy. Birkhäuser Verlag, Basel, pp 63–116

Christensen RL, Kohler BE (1973) Low resolution optical spectroscopy of retinyl polyenes: low lying electronic levels and spectral broadness. Photochem Photobiol 1973:293–301

Cleland WW, Frey PA, Gerlt JA (1998) The low barrier hydrogen bond in enzymatic catalysis. J Biol Chem 273:25529–25532

Dioumaev AK, Wang JM, Bálint Z, Váró G, Lanyi JK (2003) Proton transport by proteorhodopsin requires that the retinal Schiff base counterion Asp-97 be anionic. Biochemistry 42:6582–6587

Dioumaev AK, Wang JM, Lanyi JK (2010) Low-temperature FTIR study of multiple K intermediates in the photocycles of bacteriorhodopsin and xanthorhodopsin. J Phys Chem B 114:2920–2931

Drachev LA, Frolov VN, Kaulen AD, Liberman EA, Ostroumov SA, Plakunova GV, Semenov AY, Skulachev VP (1976) Reconstitution of biological molecular generators of electric current. Bacteriorhodopsin. J Biol Chem 251:7059–7065

Frank HA, Cogdell RJ (1993) The photochemistry and function of carotenoids in photosynthesis. In: Young A, Britton G (eds) Carotenoids in photosynthesis. Chapman and Hall, London, pp 252–326

Fuhrman JA, Schwalbach MS, Stingl U (2008) Proteorhodopsins: an array of physiological roles? Nat Rev Microbiol 6:488–494

Fujimoto KJ, Hayashi S (2009) Electronic Coulombic coupling of excitation-energy transfer in xanthorhodopsin. J Am Chem Soc 131:14152–14153

Garczarek F, Brown LS, Lanyi JK, Gerwert K (2005) Proton binding within a membrane protein by a protonated water cluster. Proc Natl Acad Sci USA 102:3633–3638

Georgakopoulou S, Cogdell RJ, van Grondelle R, van Amerongen H (2003) Linear-dichroism measurements on the LH2 antenna complex of *Rhodopseudomonas acidophila* strain 10050 show that the transition dipole moment of the carotenoid rhodopin glucoside is not collinear with the long molecular axis. J Phys Chem B 107:655–658

Georgakopoulou S, van Grondelle R, van der Zwan G (2004) Circular dichroism of carotenoids in bacterial light-harvesting complexes: experiments and modeling. Biophys J 87:3010–3022

Giovannoni SJ, Hayakawa DH, Tripp HJ, Stingl U, Givan SA, Cho J-C, Oh H-M, Kitner JB, Vergin KL, Rappé MS (2008) The small genome of an abundant coastal ocean methylotroph. Environ Microbiol 10:1771–1782

Gomez-Consarnau L, Gonzalez JM, Coll-Llado M, Gourdon P, Pascher T, Neutze R, Pedros-Alio C, Pinhassi J (2007) Light stimulates growth of proteorhodopsin-containing marine Flavobacteria. Nature 445:210–213

Hirai T, Subramaniam S, Lanyi JK (2009) Structural snapshots of conformational changes in a seven-helix membrane protein: lessons from bacteriorhodopsin. Curr Opin Struct Biol 19: 433–439

Imasheva ES, Balashov SP, Wang JM, Dioumaev AK, Lanyi JK (2004) Selectivity of retinal photoisomerization in proteorhodopsin is controlled by aspartic acid 227. Biochemistry 43: 1648–1655

Imasheva ES, Shimono K, Balashov SP, Wang JM, Zadok U, Sheves M, Kamo N, Lanyi JK (2005) Formation of a long-lived photoproduct with a deprotonated Schiff base in proteorhodopsin, and its enhancement by mutation of Asp227. Biochemistry 44:10828–10838

Imasheva ES, Balashov SP, Wang JM, Lanyi JK (2006) pH-dependent transitions in xanthorhodopsin. Photochem Photobiol 82:1406–1413

Imasheva ES, Balashov SP, Wang JM, Smolensky E, Sheves M, Lanyi JK (2008) Chromophore interaction in xanthorhodopsin – retinal dependence of salinixanthin binding. Photochem Photobiol 84:977–984

Imasheva ES, Balashov SP, Choi AR, Jung K-H, Lanyi JK (2009) Reconstitution of *Gloeobacter violaceus* rhodopsin with a light-harvesting carotenoid antenna. Biochemistry 48:10948–10955

Imasheva ES, Balashov SP, Wang JM, Lanyi JK (2011) Removal and reconstitution of the carotenoid antenna of xanthorhodopsin. J Membr Biol 239:95–104

Ke B, Imsgard F, Kjosen H, Liaaen-Jensen S (1970) Electronic spectra of carotenoids at 77°K. Biochim Biophys Acta 210:139–152

Kralj JM, Bergo VB, Amsden JJ, Spudich EN, Spudich JL, Rothschild KJ (2008) Protonation state of Glu142 differs in the green- and blue-absorbing variants of proteorhodopsin. Biochemistry 47:3447–3453

Krueger BP, Scholes GD, Fleming GR (1998) Calculation of couplings and energy-transfer pathways between the pigments of LH2 by the ab initio transition density cube method. J Phys Chem B 102:5378–5386

Lanyi JK, Balashov SP (2008) Xanthorhodopsin: a bacteriorhodopsin-like proton pump with a carotenoid antenna. Biochim Biophys Acta 1777:684–688

Litvin FF, Balashov SP, Sineshchekov VA (1975) The investigation of the primary photochemical conversions of bacteriorhodopsin in purple membranes and cells of *Halobacterium halobium* by the low temperature spectrophotometry method. Bioorgan Khim 1:1767–1777

Litvin FF, Boichenko VA, Balashov SP, Dubrovskii VT (1977) Photoinduced inhibition and stimulation of respiration in cells of *Halobacterium halobium*: kinetics, action spectra, relation to photoinduction of Δ_pH. Biofizika 22:1062–1071

Lozier RH, Bogomolni RA, Stoeckenius W (1975) Bacteriorhodopsin: a light-driven proton pump in *Halobacterium halobium*. Biophys J 15:955–963

Luecke H, Richter H-T, Lanyi JK (1998) Proton transfer pathways in bacteriorhodopsin at 2.3 Angstrom resolution. Science 280:1934–1937

Luecke H, Schobert B, Richter H-T, Cartailler J-P, Lanyi JK (1999a) Structural changes in bacteriorhodopsin during ion transport at 2 Angstrom resolution. Science 286:255–260

Luecke H, Schobert B, Richter H-T, Cartailler J-P, Lanyi JK (1999b) Structure of bacteriorhodopsin at 1.55 Å resolution. J Mol Biol 291:899–911

Luecke H, Schobert B, Stagno J, Imasheva ES, Wang JM, Balashov SP, Lanyi JK (2008) Crystallographic structure of xanthorhodopsin, the light-driven proton pump with a dual chromophore. Proc Natl Acad Sci USA 105:16561–16565

Lutnaes BF, Oren A, Liaaen-Jensen S (2002) New C_{40}-carotenoid acyl glycoside as principal carotenoid in *Salinibacter ruber*, an extremely halophilic eubacterium. J Nat Prod 65: 1340–1343

Maeda A, Verhoeven MA, Lugtenburg J, Gennis RB, Balashov SP, Ebrey TG (2004) Water rearrangement around the Schiff base in the late K (KL) intermediate of the bacteriorhodopsin photocycle. J Phys Chem B 108:1096–1101

McDermott G, Prince SM, Freer AA, Hawthornthwaite-Lawless AM, Papiz MZ, Cogdell RJ, Isaacs NW (1995) Crystal structure of an integral membrane light-harvesting complex from photosynthetic bacteria. Nature 374:517–521

Michel H, Oesterhelt D (1980) Light-induced changes of the pH gradient and the membrane potential in *Halobacterium halobium*. FEBS Lett 65:175–178

Ming M, Lu M, Balashov SP, Ebrey TG, Li QG, Ding JD (2006) pH dependence of light-driven proton pumping by an archaerhodopsin from Tibet: comparison with bacteriorhodopsin. Biophys J 90:3322–3332

Miranda MRM, Choi AR, Shi L, Bezerra AG, Jung K-H, Brown LS (2009) The photocycle and proton translocation pathway in a cyanobacterial ion-pumping rhodopsin. Biophys J 96: 1471–1481

Mongodin EF, Nelson KE, Daugherty S, DeBoy RT, Wister J, Khouri H, Weidman J, Walsh DA, Papke RT, Sanchez Perez G, Sharma AK, Nesbø CL, MacLeod D, Bapteste E, Doolittle WF,

Charlebois RL, Legault B, Rodriguez-Valera F (2005) The genome of *Salinibacter ruber*: convergence and gene exchange among hyperhalophilic bacteria and archaea. Proc Natl Acad Sci USA 102:18147–18152

Mukohata Y, Ihara K, Uegaki K, Miyashita Y, Sugiyama Y (1991) Australian *Halobacteria* and their retinal-protein ion pumps. Photochem Photobiol 54:1039–1045

Oesterhelt D (1998) The structure and mechanism of the family of retinal proteins from halophilic archaea. Curr Opin Cell Biol 8:489–500

Oesterhelt D, Stoeckenius W (1973) Functions of a new photoreceptor membrane. Proc Natl Acad Sci USA 70:2853–2857

Peña A, Valens M, Santos F, Buczolits S, Antón J, Kämpfer P, Busse H-J, Amann R, Rosselló-Mora R (2005) Intraspecific comparative analysis of the species *Salinibacter ruber*. Extremophiles 9:151–161

Petrovskaya LE, Lukashev EP, Chupin VV, Sychev SV, Lyukmanova EN, Kryukova EA, Ziganshin RH, Spirina EV, Rivkina EM, Khatypov RA, Erokhina LG, Gilichinsky DA, Shuvalov VA, Kirpichnikov MP (2010) Predicted bacteriorhodopsin from *Exiguobacterium sibiricum* is a functional proton pump. FEBS Lett 584:4193–4196

Polívka T, Frank HA (2010) Molecular factors controlling photosynthetic light harvesting by carotenoids. Acc Chem Res 43:1125–1134

Polívka T, Sundström V (2004) Ultrafast dynamics of carotenoid excited states – from solution to natural and artificial systems. Chem Rev 104:2021–2071

Polívka T, Balashov SP, Chábera P, Imasheva ES, Yartsev A, Sundström V, Lanyi JK (2009) Femtosecond carotenoid to retinal energy transfer in xanthorhodopsin. Biophys J 96: 2268–2277

Rothschild KJ, Roepe P, Gillespie J (1985) Fourier transform infrared spectroscopic evidence for the existence of two conformations of the bacteriorhodopsin primary photoproduct at low temperature. Biochim Biophys Acta 808:140–148

Schobert B, Lanyi JK (1982) Halorhodopsin is a light-driven chloride pump. J Biol Chem 257: 10306–10313

Schobert B, Brown LS, Lanyi JK (2003) Crystallographic structures of the M and N intermediates of bacteriorhodopsin: assembly of a hydrogen-bonded chain of water molecules between Asp-96 and the retinal Schiff base. J Mol Biol 330:553–570

Scholes GD (2003) Long-range resonance energy transfer in molecular systems. Annu Rev Phys Chem 54:57–87

Sharma AK, Zhaxybayeva O, Papke RT, Doolitle WF (2008) Actinorhodopsins: proteorhodopsin-like gene sequences found predominantly in non-marine environments. Environ Microbiol 10:1039–1056

Sharma AK, Sommerfeld K, Bullerjahn GS, Matteson AR, Wilhelm SW, Jezbera J, Brandt U, Doolittle WF, Hahn MW (2009) Actinorhodopsin genes discovered in diverse freshwater habitats and among cultivated freshwater *Actinobacteria*. ISME J 3:726–737

Smolensky E, Sheves M (2009) Retinal-salinixanthin interactions in xanthorodopsin: a circular dichroism (CD) spectroscopy study with artificial pigments. Biochemistry 48:8179–8188

Spudich JL, Jung K-H (2005) Microbial rhodopsins: phylogenetic and functional diversity. In: Briggs WR, Spudich JL (eds) Handbook of photosensory receptors. Wiley-VCH, Darmstadt, pp 1–23

Venter JC, Remington K, Heidelberg JF, Halpern AL, Rusch D, Eisen JA, Wu D, Paulsen I, Nelson KE, Nelson W, Fouts DE, Levy S, Knap AH, Lomas MW, Nealson K, White O, Peterson J, Hoffman J, Parsons R, Baden-Tillson H, Pfannkoch C, Rogers Y-H, Smith HO (2004) Environmental genome shotgun sequencing of the Sargasso Sea. Science 304:66–74

Yoshimura K, Kouyama T (2008) Structural role of bacterioruberin in the trimeric structure of archaerhodopsin-2. J Mol Biol 375:1267–1281

Zhu JY, Gdor I, Smolensky E, Friedman N, Sheves M, Ruhman S (2010) Photoselective ultrafast investigation of xanthorhodopsnin and its carotenoid antenna salinixanthin. J Phys Chem B 114:3038–3045